

# Tetranuclear [MDy]<sub>2</sub> Compounds and Their Dinuclear [MDy] (M = Zn/Cu) Building Units: Their Assembly, Structures, and Magnetic Properties

Peng Zhang,<sup>†,‡</sup> Li Zhang,<sup>†,§</sup> Shuang-Yan Lin,<sup>†,‡</sup> and Jinkui Tang<sup>\*,†</sup>

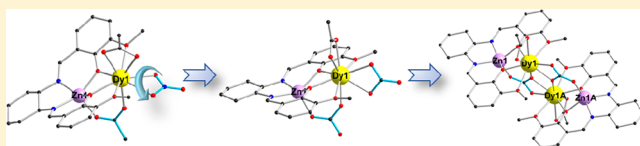
<sup>†</sup>State Key Laboratory of Rare Earth Resource Utilization, Changchun Institute of Applied Chemistry, Chinese Academy of Sciences, Changchun 130022, P. R. China

<sup>‡</sup>University of Chinese Academy of Sciences, Beijing, 100039, P. R. China

<sup>§</sup>College of Chemistry and Chemical Engineering, Inner Mongolia University, Hohhot 010021, P. R. China

## Supporting Information

**ABSTRACT:** The reactions between a salen ligand *N,N'*-bis(3-methoxysalicylidene)-1,2-cyclohexanediamine (H<sub>2</sub>L) and different metal salts lead to the formation of four 3d-4f [MDy] and [MDy]<sub>2</sub> (M = Zn/Cu) compounds, where the [MDy]<sub>2</sub> can be considered as resulting from the assembly of two [MDy] building blocks. Field-induced single molecule magnet (SMM) behavior was observed in [ZnDy] and [CuDy] compounds with the effective suppression of fast quantum tunneling under a dc field. Moreover, the [ZnDy]<sub>2</sub> compound demonstrates typical SMM behavior, which may originate from the high axial anisotropy of Dy ions correlating to the change of coordination geometry and enhanced ferromagnetic interactions between Dy ions via the coupling of two [DyZn] units. The result suggests the positive effects of coupling blocking units to enhance their SMM behavior, presenting a promising strategy for constructing efficient heterometallic SMMs.



## INTRODUCTION

Synthesis of single molecule magnets (SMMs)<sup>1</sup> containing lanthanide ions has been an important topic in the field of molecule-based magnetic materials in recent years because of the large inherent anisotropy of most lanthanide ions.<sup>2,3</sup> A typical example is the successful enhancement of magnetic anisotropy through the deliberate incorporation of the anisotropic Dy ion, creating a new [Mn<sub>18</sub>Dy] aggregate that displays slow relaxation of magnetization.<sup>4,5</sup> Since the first discovery of SMM behavior in 3d-4f complex (a Cu<sub>2</sub>Tb<sub>2</sub> compound),<sup>3</sup> research into heterometallic complexes has been developed as a significant branch in the field of SMMs with a flood of 3d-4f complexes, containing Mn-Ln,<sup>6,7</sup> Cu-Ln,<sup>8,9</sup> Fe-Ln,<sup>10,11</sup> Ni-Ln<sup>12–14</sup> and Co-Ln<sup>15–17</sup> behaving as SMMs. In fact, the magnetic investigations of 3d-4f compounds, mainly for 3d-Gd<sup>III</sup> compounds, can date back to 1985, when the ferromagnetic interaction was discovered between Cu<sup>II</sup> and Gd<sup>III</sup> by Gatteschi et al.<sup>18,19</sup> Furthermore, the magnetocaloric application has also been explored recently in multinuclear 3d-4f clusters, such as [Ni<sub>6</sub>Gd<sub>6</sub>P<sub>6</sub>],<sup>20</sup> [Gd<sub>36</sub>Ni<sub>12</sub>]<sup>21</sup> and other 3d-4f complexes.<sup>22–24</sup> In addition, it is noted that the design of multifunctional magnetic materials<sup>25</sup> combining the magnetism and other functions such as luminescence or chirality has become an important focus of interest in this field.<sup>26–30</sup> Here the heterometallic complexes have presented a great promise in magneto-luminescent molecular material.<sup>31,32</sup> Therefore, the construction of compounds incorporating both transition metal and lanthanide ions represents a promising field of research in molecule-based magnetic materials.

To date, some empirically methodologies to obtain a variety of heterometallic complexes have been established, such as the employment of compartmental or multifunctional ligands.<sup>33–35</sup> In general, the design of ligands containing different coordination donors and bonding modes is considered as a critical factor in determining crystal structure of a heterometallic complex.<sup>19,36</sup> However it should be noted that some subordinate factors, such as the nature of anions, the radii of metal ions, and the introduction of secondary ligands, also play a vital role in the assembly of coordination compounds.<sup>37–40</sup> In this context, four new compounds (ZnDy, **1**; [ZnDy]<sub>2</sub>, **2**; CuDy, **3**; [CuDy]<sub>2</sub>, **4**) were obtained through using a “salen” type Schiff-base ligands (H<sub>2</sub>L), representing a successful assembly of [MDy]<sub>2</sub> compounds based on [MDy] (M = Zn/Cu) units mediated by anions (ClO<sub>4</sub><sup>−</sup>). Here field-induced slow relaxation of magnetization is observed in the ZnDy (**1**) and CuDy (**3**) compounds. Remarkably, the [ZnDy]<sub>2</sub> (**2**) compound bridged by two CO<sub>3</sub><sup>2−</sup> displays typical SMM behavior, possibly influenced by the ferromagnetic interactions between lanthanide ions concomitant with variation of the axial geometry around Dy ions through the assembly of two building blocks, while no SMM behavior was observed in [CuDy]<sub>2</sub> (**4**) complex bridged by two OH<sup>−</sup> groups.

**Received:** March 13, 2013

Table 1. Details of the Structure Solution and Refinement of Complexes 1–4

	1	2	3	4
formula	C <sub>27</sub> H <sub>34</sub> DyN <sub>3</sub> O <sub>12</sub> Zn	C <sub>60</sub> H <sub>94</sub> Dy <sub>2</sub> N <sub>4</sub> O <sub>28</sub> Zn <sub>2</sub>	C <sub>26</sub> H <sub>30</sub> CuDyN <sub>3</sub> O <sub>11</sub>	C <sub>50</sub> H <sub>78</sub> Cl <sub>4</sub> Cu <sub>2</sub> Dy <sub>2</sub> N <sub>4</sub> O <sub>34</sub>
<i>M<sub>r</sub></i>	820.44	1775.13	786.57	1873.04
color	pale-yellow	pale-yellow	dark green	brown
crystal size [mm]	0.21 × 0.20 × 0.18	0.20 × 0.16 × 0.15	0.22 × 0.20 × 0.19	0.19 × 0.17 × 0.16
crystal system	triclinic	triclinic	triclinic	triclinic
space group	<i>P</i> $\bar{1}$	<i>P</i> $\bar{1}$	<i>P</i> $\bar{1}$	<i>P</i> $\bar{1}$
<i>T</i> [K]	185(2)	185(2)	185(2)	185(2)
<i>a</i> [Å]	8.6421(5)	12.2311(6)	8.5160(5)	10.6912(7)
<i>b</i> [Å]	13.3663(7)	12.5430(6)	12.8301(8)	12.5528(8)
<i>c</i> [Å]	13.8293(8)	13.6239(7)	13.8385(9)	13.4070(8)
$\alpha$ [deg]	91.6820(10)	71.8110(10)	82.4100(10)	100.7830(10)
$\beta$ [deg]	97.5110(10)	64.7270(10)	74.4400(10)	92.2780(10)
$\gamma$ [deg]	108.6700(10)	89.4210(10)	74.9300(10)	104.5300(10)
<i>V</i> [Å <sup>3</sup> ]	1496.10(15)	1777.06(15)	1403.34(15)	1703.85(19)
<i>Z</i>	2	1	2	1
$\rho_{\text{calcd}}$ [g cm <sup>−3</sup> ]	1.821	1.659	1.861	1.825
$\mu(\text{Mo-K}\alpha)$ [mm <sup>−1</sup> ]	3.347	2.828	3.465	3.033
<i>F</i> (000)	818	898	780	936
reflins collected	8344	9904	7861	9523
unique reflins	5880	6977	5502	6701
<i>R</i> <sub>int</sub>	0.0169	0.0200	0.0220	0.0256
parameters/restraints	403/12	446/0	383/0	440/12
GOF	1.042	1.069	1.036	1.037
<i>R</i> <sub>1</sub> [ <i>I</i> > 2σ( <i>I</i> )]	0.0329	0.0324	0.0288	0.0428
<i>wR</i> <sub>2</sub> (all data)	0.0802	0.0827	0.0717	0.0977
largest diff. peak/hole [e Å <sup>−3</sup> ]	1.375 and −0.883	1.134 and −0.944	1.063 and −1.097	1.046 and −0.631

## EXPERIMENTAL SECTION

**General Procedures.** All chemicals were of analytical reagent grade and were used as received without any further purification. Elemental analysis for C, H, and N were performed on a Perkin-Elmer 2400 analyzer. IR spectra were recorded with a Perkin-Elmer Fourier transform infrared spectrophotometer with samples prepared as KBr disks in the 4000–300 cm<sup>−1</sup> range.

**X-ray Crystal Structure Determinations.** Single crystal X-ray data of the title complexes were collected at 185 (2) K on a Bruker Apex II CCD diffractometer equipped with graphite-monochromatized Mo- $\text{K}\alpha$  radiation ( $\lambda = 0.71073$  Å). Data processing was completed with the SAINT processing program. The structures were solved by direct methods and refined by full matrix least-squares methods on *F*<sup>2</sup> using SHELXTL-97.<sup>41</sup> The locations of the heaviest atoms (Dy, Zn, and Cu) were easily determined, and C, O, N, and Cl atoms were determined from the difference Fourier maps. The nonhydrogen atoms were refined anisotropically. All hydrogen atoms were introduced in calculated positions and refined with fixed geometry with respect to their carrier atoms. Crystallographic data are summarized in Table 1. CCDC 905911–905914 contain the supplementary crystallographic data for this paper. These data can be obtained free of charge from The Cambridge Crystallographic Data Centre via [www.ccdc.cam.ac.uk/data\\_request/cif](http://www.ccdc.cam.ac.uk/data_request/cif).

**Magnetic Measurements.** Magnetic susceptibility measurements were recorded on a Quantum Design MPMS-XL7 SQUID magnetometer equipped with a 7 T magnet. The variable-temperature magnetization was measured with an external magnetic field of 1000 Oe in the temperature range of 1.9–300 K. Diamagnetic corrections for the compounds were estimated from the Pascal's constants,<sup>42</sup> and magnetic data were corrected for diamagnetic contributions of the sample holder.

**Synthesis of H<sub>2</sub>L.** The Schiff-base ligand was synthesized by a condensation reaction between 1,2-cyclohexanediamine (1.150 g, 10 mmol) and *o*-vanillin (3.040 g, 20 mmol) in methanol (50 mL).<sup>43</sup>

**Synthesis of [DyZnL(OAc)<sub>2</sub>(NO<sub>3</sub>)]·CH<sub>3</sub>OH (1).** H<sub>2</sub>L (0.1 mmol, 0.038 g) was dissolved in CH<sub>3</sub>OH/CH<sub>3</sub>CN (10 mL/5 mL) followed

by the addition of Dy(NO<sub>3</sub>)<sub>3</sub>·6H<sub>2</sub>O (0.1 mmol, 0.046 g) and triethylamine (0.2 mmol, 0.028 mL). Then Zn(OAc)<sub>2</sub>·2H<sub>2</sub>O (0.1 mmol, 0.022 g) was added after 2 h, and the resulting solution was stirred for 3 h. Pale yellow rectangular single crystals, suitable for X-ray diffraction analysis, were formed after one week. Yield: 30 mg (37%, based on the metal salt). Elemental analysis (%) calcd for C<sub>27</sub>H<sub>34</sub>DyN<sub>3</sub>O<sub>12</sub>Zn: C, 39.52, H, 4.18, N, 5.12; found: C, 39.55, H, 4.05, N, 5.23. IR (KBr, cm<sup>−1</sup>): 3438 (br), 2943 (w), 2865 (w), 1655 (m), 1631 (s), 1607 (m), 1557 (s), 1476 (s), 1455 (s), 1396 (m), 1355 (w), 1305 (s), 1243 (m), 1222 (s), 1168(w), 1078 (m), 1037 (w), 1023 (m), 963 (m), 952 (m), 854 (w), 782 (w), 742 (s), 665 (m), 622 (w), 566 (w), 441 (w), 424 (w).

**Synthesis of [Dy<sub>2</sub>Zn<sub>2</sub>L<sub>2</sub>(OAc)<sub>2</sub>(CO<sub>3</sub>)<sub>2</sub>]·10CH<sub>3</sub>OH (2).** H<sub>2</sub>L (0.1 mmol, 0.038 g) was dissolved in CH<sub>3</sub>OH/CH<sub>2</sub>Cl<sub>2</sub> (10 mL/10 mL) followed by the addition of Dy(ClO<sub>4</sub>)<sub>3</sub>·6H<sub>2</sub>O (0.1 mmol, 0.057 g) and triethylamine (0.2 mmol, 0.028 mL). Then Zn(OAc)<sub>2</sub>·2H<sub>2</sub>O (0.1 mmol, 0.022 g) was added after 2 h and the resulting solution was stirred for 3 h. Pale yellow block-shaped single crystals, suitable for X-ray diffraction analysis, were formed after 9 days. Yield: 26 mg (29%, based on the metal salt). Elemental analysis (%) calcd for C<sub>60</sub>H<sub>94</sub>Dy<sub>2</sub>N<sub>4</sub>O<sub>28</sub>Zn<sub>2</sub>: C, 40.59, H, 5.34, N, 3.16; found: C, 40.74, H, 5.23, N, 3.32. IR (KBr, cm<sup>−1</sup>): 3513 (br), 3061 (w), 2929 (m), 2859 (w), 1660 (s), 1637 (s), 1605 (s), 1565 (s), 1471 (s), 1399(s), 1358 (m), 1307 (m), 1285 (s), 1244 (s), 1218 (s), 1167(m), 1078 (s), 1023 (m), 975 (m), 950 (m), 919 (w), 851 (m), 785 (w), 737 (s), 668 (m), 622 (s), 580 (w), 554 (w), 514 (w), 459 (w), 424 (m).

**Synthesis of [DyCuL(OAc)<sub>2</sub>(NO<sub>3</sub>)] (3).** A procedure similar to that for 1 was followed except that Zn(OAc)<sub>2</sub>·2H<sub>2</sub>O and CH<sub>3</sub>OH/CH<sub>3</sub>CN (10 mL/5 mL) were replaced by Cu(OAc)<sub>2</sub>·H<sub>2</sub>O (0.1 mmol, 0.020 g) and CH<sub>3</sub>OH/CH<sub>2</sub>Cl<sub>2</sub> (10 mL/10 mL), respectively. Dark green rectangular single crystals, suitable for X-ray diffraction analysis, were formed after 6 days. Yield: 32 mg (41%, based on the metal salt). Elemental analysis (%) calcd for C<sub>26</sub>H<sub>30</sub>CuDyN<sub>3</sub>O<sub>11</sub>: C, 39.70, H, 3.84, N, 5.34; found: C, 39.42, H, 3.78, N, 5.48. IR (KBr, cm<sup>−1</sup>): 3422 (br), 3071 (w), 2945 (w), 2862 (w), 1637 (s), 1608 (m), 1577 (s), 1561 (m), 1477 (s), 1459 (s), 1417 (s), 1391 (m), 1347 (m), 1307 (s), 1290 (s), 1248 (m), 1224 (s), 1165(w), 1073 (m), 1039 (w), 965

(m), 922 (w), 855 (w), 783 (w), 742 (s), 683 (w), 650 (w), 619 (w), 565 (w), 458 (w), 427 (w).

**Synthesis of  $[\text{Dy}_2\text{Cu}_2\text{L}_2(\mu_2\text{-OH})_2(\text{H}_2\text{O})_2(\text{CH}_3\text{OH})_2](\text{ClO}_4)_4 \cdot 4\text{CH}_3\text{OH}$  (4).** A procedure similar to that for **2** was followed except that  $\text{Zn}(\text{OAc})_2 \cdot 2\text{H}_2\text{O}$  and  $\text{CH}_3\text{OH}/\text{CH}_2\text{Cl}_2$  (10 mL/10 mL) were replaced by  $\text{Cu}(\text{ClO}_4)_2 \cdot 6\text{H}_2\text{O}$  (0.1 mmol, 0.037 g) and  $\text{CH}_3\text{OH}/\text{CH}_2\text{Cl}_2$  (10 mL/5 mL), respectively. Brown block-shaped single crystals, suitable for X-ray diffraction analysis, were formed after 8 days. Yield: 20 mg (21%, based on the metal salt). Elemental analysis (%) calcd for  $\text{C}_{50}\text{H}_{78}\text{Cl}_4\text{Cu}_2\text{Dy}_2\text{N}_4\text{O}_{34}$ : C, 32.06, H, 4.20, N, 2.99; found: C, 32.11, H, 4.07, N, 3.05. IR (KBr,  $\text{cm}^{-1}$ ): 3410 (br), 2949 (w), 2851 (w), 1633 (s), 1609 (m), 1558 (w), 1475 (s), 1458 (s), 1443 (m), 1392 (w), 1346 (w), 1308 (s), 1289 (m), 1240 (m), 1222 (s), 1172 (m), 1074 (s), 952 (m), 930 (w), 857 (w), 783 (w), 741 (m), 670 (w), 651 (w), 623 (m), 589 (w), 564 (w), 469 (w), 448 (m), 425 (w).

## RESULTS AND DISCUSSION

**Synthetic Aspects.** For *o*-vanillin salen ligands, it tends to form the binuclear Ln-M complex (M = transition metal), which is the result of the fact that the inner site (commonly of the  $\text{N}_2\text{O}_2$  type) shows preference for transition metal ions and the outer site ( $\text{O}_4$ ) shows preference for lanthanide ions, as indicated by many examples.<sup>12,44–46</sup> In addition, many transition metal salen complexes act as highly useful building blocks for the design of magnetic assemblies not only toward bulk magnets but also toward molecular superparamagnets.<sup>47</sup> Very recently, a carbonate-bridged  $\text{Ni}_2\text{Gd}_2$  complex was assembled by atmospheric  $\text{CO}_2$  fixation, where a ferromagnetic interaction can be observed.<sup>48</sup> Thus, we were motivated to explore the possibility of obtaining novel heterometallic SMM systems containing such heterometallic building blocks.

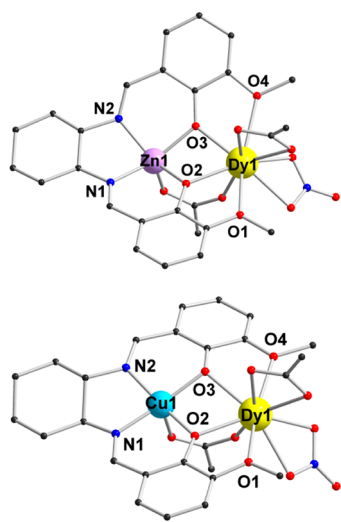


**Figure 1.** Molecular structures of **1** (up) and **3** (bottom). Hydrogen atoms and solvent molecules are omitted for clarity. Color scheme: yellow, Dy; purple, Zn; sky blue, Cu; red, O; blue, N; gray, C.

First, the  $[\text{ZnDy}]$  (**1**, Figure 1) and  $[\text{ZnDy}]_2$  (**2**, Figure 2) compounds were obtained through the reactions of salen ligand ( $\text{H}_2\text{L}$ ) with different metal salts under the same base conditions (Scheme 1). A careful inspection of experimental condition reveals that the anion ( $\text{ClO}_4^-$ ) provided by the lanthanide salt may have a dominant contribution to the coupling of  $\text{ZnDy}$  (**1**) units, forming  $[\text{ZnDy}]_2$  (**2**) complex, which might mainly hinge on the weakly coordinating ability of  $\text{ClO}_4^-$  to lanthanide ions.

In most examples, the perchloride anion tends not to coordinate with lanthanide ion or provides only one coordinated site,<sup>38,49,50</sup> which give a chance for the introduction of other ligands with strong bridging ability, such as  $\text{CO}_3^{2-}$  from the fixation of atmospheric  $\text{CO}_2$  and  $\text{OH}^-$  from  $\text{H}_2\text{O}$ . Subsequently, the  $[\text{CuDy}]_2$  (**4**) compound was also obtained through the reaction between ligand  $\text{H}_2\text{L}$  and perchlorate salts ( $\text{Cu}(\text{ClO}_4)_2$  and  $\text{Dy}(\text{ClO}_4)_3$ ) under same conditions, further confirming our deduction.

**Crystal Structures.** The reactions of  $\text{Dy}(\text{NO}_3)_3 \cdot 6\text{H}_2\text{O}$ ,  $\text{Zn}(\text{OAc})_2 \cdot 2\text{H}_2\text{O}/\text{Cu}(\text{OAc})_2 \cdot \text{H}_2\text{O}$  and  $\text{Et}_3\text{N}$  in a 1:1:2 ratio afford pale yellow and dark green crystals, namely,  $[\text{DyML}(\text{OAc})_2(\text{NO}_3)] \cdot n\text{CH}_3\text{OH}$  [M =  $\text{Zn}^{\text{II}}$  with  $n = 1$  (**1**), M =  $\text{Cu}^{\text{II}}$  with  $n = 0$  (**3**)]. However, the reactions of  $\text{Dy}(\text{ClO}_4)_3 \cdot 6\text{H}_2\text{O}$ ,  $\text{Zn}(\text{OAc})_2 \cdot 2\text{H}_2\text{O}/\text{Cu}(\text{ClO}_4)_2 \cdot 6\text{H}_2\text{O}$  and  $\text{Et}_3\text{N}$  in a 1:1:2 ratio in mixed solvent (methanol/dichloromethane) afford pale yellow and brown crystals,  $[\text{Dy}_2\text{Zn}_2\text{L}_2(\text{OAc})_2(\text{CO}_3)_2] \cdot 10\text{CH}_3\text{OH}$  (**2**) and  $[\text{Dy}_2\text{Cu}_2\text{L}_2(\mu_2\text{-OH})_2(\text{H}_2\text{O})_2(\text{CH}_3\text{OH})_2](\text{ClO}_4)_4 \cdot 4\text{CH}_3\text{OH}$  (**4**). Details for the structure solution and refinement are summarized in Table 1, and selected bond distances and angles are listed in Supporting Information, Table S1.

Single-crystal X-ray studies revealed that **1** and **3** are isostructural, crystallizing in the triclinic space group  $P\bar{1}$  with  $Z = 2$ . A perspective view of the molecular structures of **1** and **3** is presented in Figure 1. In the asymmetric molecule, M ions (M =  $\text{Zn}^{\text{II}}$  for **1** and  $\text{Cu}^{\text{II}}$  for **3**) and  $\text{Dy}^{\text{III}}$  ions are located in the inner  $\text{N}_2\text{O}_2$  pocket and outer  $\text{O}_4$  pocket of  $\text{L}^{2-}$  ligand, respectively and are linked by two phenol oxygen atoms (O2 and O3) from  $\text{L}^{2-}$  ligand and a acetate group in a  $\eta^1:\eta^1:\mu$  fashion with the Dy–O–M angles of  $101.45^\circ$  and  $101.47^\circ$  for **1** and  $103.03^\circ$  and  $101.11^\circ$  for **3**. The coordination sphere of Dy1 is completed by bidentate acetate and nitrate anions, making nine-coordinate with a distorted tricapped trigonal prismatic (TCTP) geometry. The average Dy–O distances are in the range of  $2.302(3)$ – $2.616(3)$  Å and  $2.257(3)$ – $2.653(3)$  Å for **1** and **3**, respectively, indicating a wide distribution of bond lengths. Moreover, the bridging acetate group forces the structure to be folded with a small hinge.<sup>12</sup> The M ion is five-coordinated with the M–O distances of  $1.976(3)$ – $2.017(3)$  Å for **1** and  $1.918(3)$ – $2.242(3)$  Å for **3**, displaying a pyramidal geometry.

Both compound **2** and **4** are crystallized in the triclinic space group  $P\bar{1}$  with  $Z = 1$ , whose structures are displayed in Figures 2 and 3. In compound **2**, the asymmetric unit is composed of one  $\text{Zn}^{\text{II}}$  ion, one  $\text{Dy}^{\text{III}}$  ion, one  $\text{L}^{2-}$  ligand, one bidentate acetate anion, and one carbonate anion. The carbonate anion binds one  $\text{Zn}^{\text{II}}$  ion and two  $\text{Dy}^{\text{III}}$  ions in  $\eta^1:\eta^2:\eta^1:\mu_3$  bridging mode. Actually, complex **2** can be considered as the coupling of two  $[\text{ZnDy}]$  units through the loss of terminal nitrate and bridging acetate groups and formation of bridging carbonate involving the fixation of atmospheric  $\text{CO}_2$  (Figure 2). In fact, such a situation is not unprecedented, and there are many examples of lanthanide complexes where the carbonate from atmospheric  $\text{CO}_2$  fixation links several lanthanide ions into a large cluster.<sup>48,51–54</sup> Such modulation allows five oxygen atoms (O1, O2, O3, O4, and O6) around Dy1 being the nearly coplanar, favoring the high axial anisotropy of  $\text{Dy}^{\text{III}}$  ion, which could be associated with the strong intramolecular magnetic interactions and SMM behavior. All  $\text{Dy}^{\text{III}}$  and  $\text{Zn}^{\text{II}}$  atoms arrange in a zigzag fashion with the Dy–O and Zn–O distances in the range of  $2.292(3)$ – $2.617(3)$  Å and  $1.977(3)$ – $2.027(3)$  Å, respectively, and Dy–O–Zn angles of  $103.61^\circ$  and  $102.27^\circ$ ,

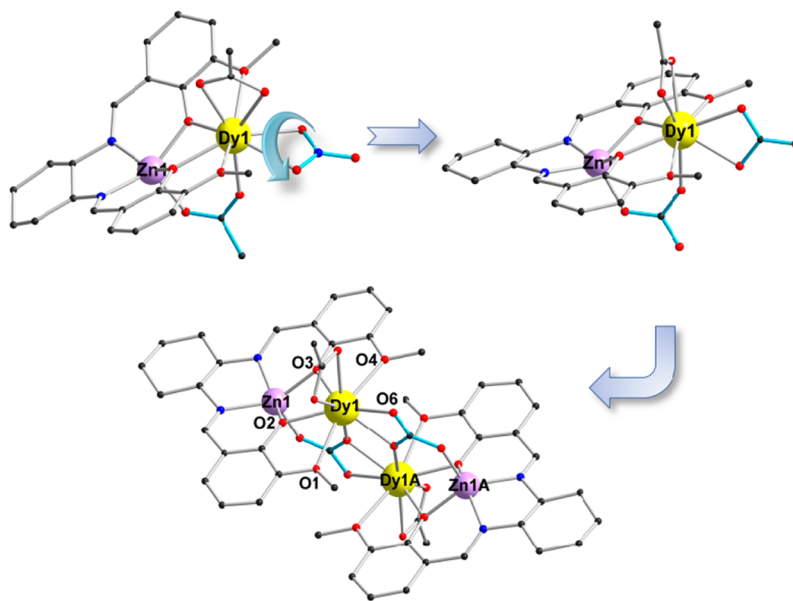


Figure 2. Crystal structure of compound 2 and its assembly from [ZnDy] building blocks (1).

**Scheme 1. Assembly Process for [ZnDy] and [ZnDy]<sub>2</sub> Compounds**

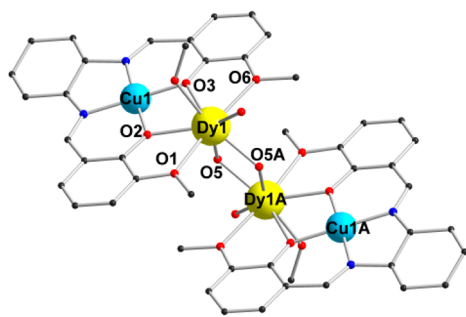
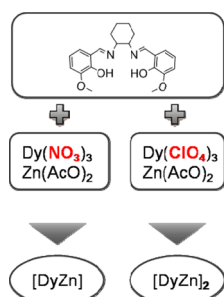


Figure 3. Crystal structure of compound 4.

which are in agreement with the corresponding values of compound 1.

In molecule 4, two  $\mu_2$ -OH anions replace two carbonato anions of 2, and play the role of connecting two Dy<sup>III</sup> ions to generate a structure coupling two CuDy units (Figure 3). One water and one methanol molecules occupy the remaining coordination sites of Dy1 instead of terminal bidentate acetate in 2 with the Dy–O–Dy angles of 112.86(14)° and Dy–O distances of 2.231(3) Å and 2.246(3) Å. The Cu<sup>II</sup> and Dy<sup>III</sup> ions are four-coordinate and eight-coordinate, respectively. The perchlorate connects to  $\mu_2$ -OH and coordinated water molecule via intermolecular hydrogen bonds O6–H22...O15<sup>#1</sup> and O5–H5A...O16<sup>#1</sup> (symmetry codes: #1,  $-x+2, -y+1, -z+2$ ). One perchlorate and two methanol molecules join coordinated water and methanol molecules from adjacent molecules via strong O6–H21...O8<sup>#2</sup>, O9–H9A...O13<sup>#3</sup>, O8–H8A...O12<sup>#4</sup>, and O7–H7...O9 (symmetry codes: #2,  $x+1, y, z$ ; #3,  $x, y-1, z$ ; #4,  $-x+1, -y+1, -z+1$ ; see Supporting Information, Table S2 for details) bonds to generate a one-dimensional chain (Figure 4).

**Magnetic Properties.** Static susceptibility measurements on polycrystalline samples of compounds 1–4 have been measured in the temperature range of 2–300 K under a direct current (dc) field of 1000 Oe (Figures 5 and 6). The room temperature value of the  $\chi_M T$  product of compound 1 is 13.8 cm<sup>3</sup> K mol<sup>−1</sup>, comparable with the expected value of 14.17 cm<sup>3</sup>

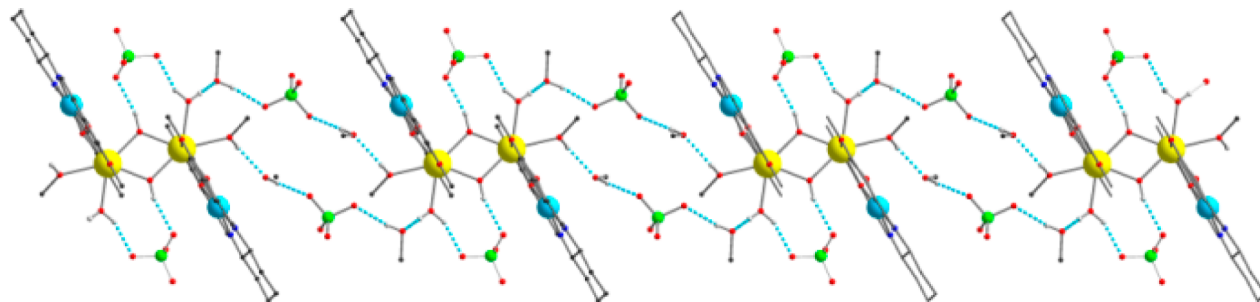
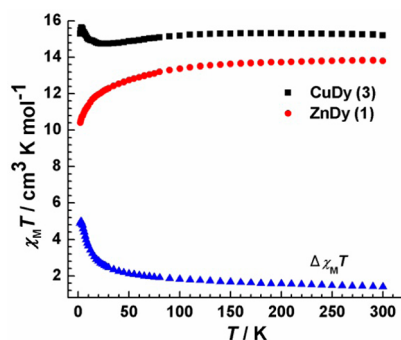


Figure 4. 1D chain of compound 4 through intermolecular hydrogen bonding.





**Figure 5.** Plots of  $\chi_M T$  vs  $T$  for complexes **1** and **3** and the difference of  $\Delta\chi_M T$ .

K mol<sup>-1</sup> for one Dy ion (<sup>6</sup>H<sub>15/2</sub>,  $g = 4/3$ ) (Figure 5). With decreasing temperature, the  $\chi_M T$  product displays a typical decrease, induced by the depopulation of the Stark sublevels of the Dy ion.<sup>55</sup> For compound **3**, the  $\chi_M T$  value of 15.2 cm<sup>3</sup> K mol<sup>-1</sup> at 300 K is compatible with the theoretical value of 14.53 cm<sup>3</sup> K mol<sup>-1</sup> for the uncoupled Cu and Dy ion (Figure 5). The value decreases slightly down to a minimum value of 14.7 cm<sup>3</sup> K mol<sup>-1</sup> with decreasing temperature, which is ascribed to the depopulation of the Stark sublevels of Dy ion, and then shows an obvious increase, reaching a maximum value of 15.6 cm<sup>3</sup> K mol<sup>-1</sup> at 3.5 K, indicating the occurrence of intramolecular ferromagnetic interactions. Finally, the  $\chi_M T$  value displays a sharp decrease below 3.5 K, probably resulting from the presence of weak intermolecular antiferromagnetic interactions. Strikingly, because compound **1** and **3** are isostructural only with some slight differences in bond lengths and angles, we can probe the nature of the magnetic interaction between Cu<sup>II</sup> and Dy<sup>III</sup> in compound **3** by extracting the  $\Delta\chi_M T$  vs  $T$  curve from the experimental  $\chi_M T$  data of compound **1** and **3**,  $\Delta\chi_M T = \chi_M T(\mathbf{3}) - \chi_M T(\mathbf{1})$  (Figure 5),<sup>56</sup> which removes the influence of the crystal-field effects of the Dy ion on dc magnetic susceptibility. Here the  $\Delta\chi_M T$  value demonstrates a constant increase with decreasing temperature in the whole temperature region, confirming a ferromagnetic interaction between Cu<sup>II</sup> and Dy<sup>III</sup> ions.<sup>12</sup>

The  $\chi_M T$  value of 30.7 cm<sup>3</sup> K mol<sup>-1</sup> at 300 K for compound **2** is a little larger than the calculated value (28.34 cm<sup>3</sup> K mol<sup>-1</sup>), while compound **4** shows a relatively reasonable value of 29.9 compared with the theoretical value of 29.06 cm<sup>3</sup> K mol<sup>-1</sup> (Figure 6). Upon cooling, the  $\chi_M T$  value of compound **2** displays a very slightly decrease to a minimum of 30.27 cm<sup>3</sup> K

mol<sup>-1</sup> at 45 K before it increases to a value of 44.0 cm<sup>3</sup> K mol<sup>-1</sup> at 2.0 K, indicating the presence of intramolecular ferromagnetic interactions. Such strong ferromagnetic interactions are rare in lanthanide-based compounds, and here its occurrence may be as a result of the connecting of two [DyZn] building blocks through two CO<sub>3</sub><sup>2-</sup> with high negative charge. The CO<sub>3</sub><sup>2-</sup> in one building block is coordinated to the Zn atom in the other building block, making the O atoms (O1, O2, O3, O4, O6) almost planar, which therefore may lead to the strong uniaxial anisotropy of the Dy ion. For **4**, the  $\chi_M T$  vs  $T$  curve demonstrates a decrease, then a little increase, and finally an abrupt drop. The decrease of  $\chi_M T$  value at the higher temperature region is associated with crystal field effects of the Dy<sup>III</sup> ion, while the magnetic behavior at low temperature should be ascribed to the competitions of magnetic interactions ( $J_{\text{Dy-Dy}}$ ,  $J_{\text{Dy-Cu}}$  and intermolecular interactions).

The  $M$ - $H$  plots measured at an applied field of 0–70 kOe for compounds **1**–**4** reveal the stronger field dependence of magnetization in compounds **2** and **3** (the initial rapid increase) than that in compounds **1** and **4** (Supporting Information, Figures S1, S2, and S3) at low field, which is in agreement with the presence of intramolecular ferromagnetic interactions in complexes **2** and **3**.<sup>57</sup> Especially for compound **2**, the value of magnetization reaches 10.1  $\mu_B$  under a small dc field of 5 kOe at 1.9 K. At high field, the magnetization for compound **1**–**4** shows a linear increase with field, finally reaching values of 6.3 (**1**), 11.8 (**2**), 7.1 (**3**), and 15.1 (**4**)  $\mu_B$  at 70 kOe and 1.9 K, but without clear saturation. Furthermore, the nonsuperimposition of the  $M$  vs  $H/T$  data on a single master curve (Figure 6 inset and Supporting Information, Figures S1, S2, S3) suggests the presence of low lying energy states and/or anisotropy in the system for compounds **1**–**4**.<sup>12,14</sup>

Variable-temperature ac susceptibility measurements as a function of temperature or frequency were carried out under zero dc field. Here only compound **2** exhibits the strong frequency-dependence of both in-phase ( $\chi'$ ) and out-of-phase ( $\chi''$ ) susceptibilities with maxima below 13 K (Figure 7), suggesting a typical SMM behavior, which is possibly associated with the strong axial anisotropy induced by coplanar coordinated O atoms around Dy ions. For compound **4**, although Dy ions show the similarly coplanar geometries, no out-of-phase signals were observed above 1.8 K (Supporting Information, Figure S4) probably because of the subtle differences in coordination environment at Dy ions or the interaction between Dy and Cu ions which might split further the ground sublevel of the Dy<sup>III</sup> ion.<sup>44,45</sup> In addition,

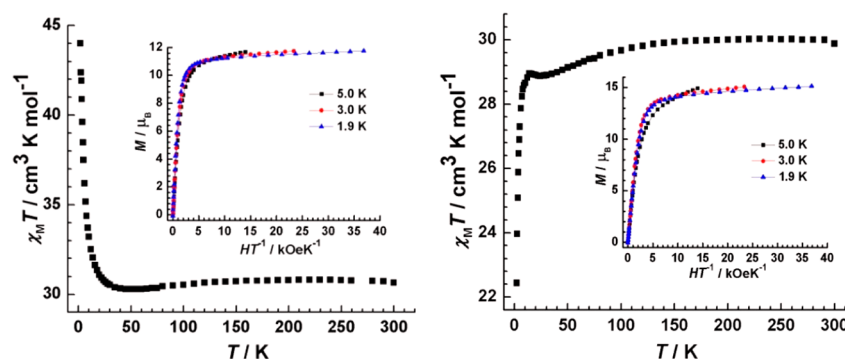


**Figure 6.** Temperature dependence of the  $\chi_M T$  product at 1000 Oe and field dependence of the magnetization at low temperatures (inset) for complexes **2** (left) and **4**. The solid lines are a guide for the eyes.

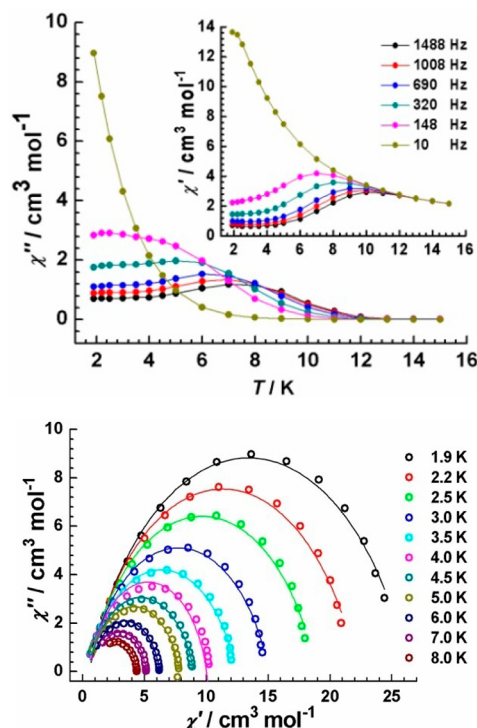


**Figure 7.** Temperature dependence of the in-phase ( $\chi'$ ) and out-of-phase ( $\chi''$ ) ac susceptibility signals for **2** under zero dc field (up). The solid lines are a guide for the eyes; Cole–Cole plots under zero-dc field for compound **2** (bottom). The solid lines indicate the fits using a generalized Debye model.

compounds **1** and **3** also show the absence of SMM behavior under zero dc field, as indicated by the temperature dependence of the ac susceptibility (Supporting Information, Figure S5), which may be attributed to the fast quantum tunneling relaxation induced by the large transverse anisotropy at local Dy sites.

From frequency dependencies of the ac susceptibility, the magnetization relaxation times ( $\tau$ ) were deduced in the temperature range of 1.9–11 K for compound **2**. Through the  $\ln \tau$  vs  $T^{-1}$  plots (Supporting Information, Figure S6), an energy barrier ( $U_{\text{eff}}$ ) of 34 K with  $\tau_0 = 2.9 \times 10^{-6}$  s can be obtained based on an Arrhenius law ( $\tau = \tau_0 \exp(U_{\text{eff}}/T)$ ) above 5 K, indicating a thermally activated mechanism at high temperature. Below 5 K, the plots show a departure from the Arrhenius behavior, which could be as a result of the quantum tunneling of magnetization (QTM). The Cole–Cole diagram ( $\chi''$  vs  $\chi'$ ) was plotted in the temperature range of 1.9–8 K (Figure 7, bottom), displaying a relatively symmetrical shape. The plots can be fitted to the generalized Debye model, with small  $\alpha$  parameters (0.14–0.22), indicating a narrow distribution of  $\tau$ .

To reduce quantum tunneling of magnetization (QTM), the optimal dc fields of 1000 and 1750 Oe according to the field dependence of ac susceptibility were applied in compound **1** and **3**, respectively (Supporting Information, Figure S7).<sup>58</sup> The application of dc field has a substantial influence on their dynamic behavior of magnetization, as seen in ac susceptibility signals. Compound **1** shows the clearly frequency-dependent signals, but no maximum in out-of-phase component ( $\chi''$ ) of ac susceptibility below 6 K (Figure 8), indicating the field-induced slow magnetic relaxation behavior. In particular, the typical SMM behavior was observed below 12 K in compound **3** with

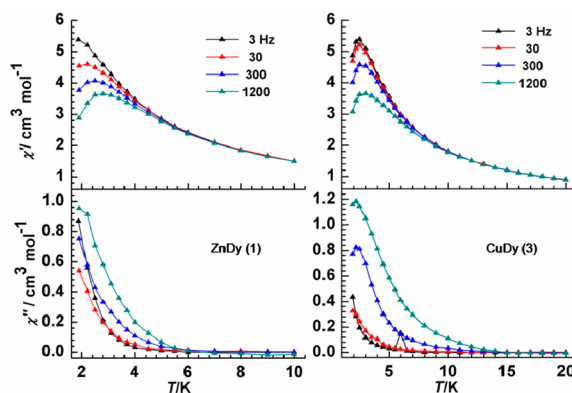


**Figure 8.** Temperature dependence of the in-phase (top) and out-of-phase (bottom) ac susceptibility signals for **1** (left) and **3** under the optimal dc field. The solid lines are a guide for the eyes.

the out-of-phase component ( $\chi''$ ) of ac susceptibility showing the maximum at the frequency of 300 and 1200 Hz (Figure 8).

In fact, a number of Ln–Zn complexes, including  $[\text{DyZn}]$ ,<sup>12,31,44</sup>  $[\text{LnZn}_3]$ ,<sup>55,59</sup>  $[\text{LnZn}_2]$ ,<sup>60,61</sup>  $[\text{Dy}_2\text{Zn}_2]$ ,<sup>62,63</sup> and  $[\text{Dy}_3\text{Zn}_2]$ ,<sup>32</sup> have been reported recently. We summarized those Ln–Zn complexes showing SMM behavior in Supporting Information, Table S3. Herein some complexes exhibit not only strong SMM behavior but also characteristic luminescent features.<sup>31</sup> It is noteworthy that the  $[\text{CeZn}_2]$  with a salen-type ligand is the first example of slow magnetic relaxation observed for  $\text{Ce}^{\text{III}}$  ion.<sup>61</sup> In addition, we can see that the SMMs in a zero-dc field are rare in those Ln–Zn complexes. In this regard, the  $\text{Dy}_2\text{Zn}_2$  compound reported in this paper behaves as a typical SMM as evidenced by the ac susceptibility data under a zero-dc field.

## CONCLUSION

Four new compounds,  $[\text{Zn}/\text{CuDy}]$  (**1**, **3**) and  $[\text{Zn}/\text{CuDy}]_2$  (**2**, **4**), have been obtained successfully through the reactions between salen ligand ( $\text{H}_2\text{L}$ ) and different metal salts. Both **1** and **3** demonstrate the field-induced slow relaxation of magnetization. Since compounds **1** and **3** are isostructural, an empirical approach developed by Costes et al.<sup>56</sup> was applied to study the nature of the magnetic interaction between Cu and Dy ion, confirming the presence of ferromagnetic interaction between them. The  $[\text{MDy}]_2$  structure can be considered as resulting from the linkage of two  $[\text{MDy}]$  units. The introduction of  $\text{CO}_3^{2-}$  leads to the transformation of highly axial coordinating geometry of Dy ion, resulting in the ferromagnetic interactions between Dy ions and SMM behavior of the compound. The results described here suggest that the assembly of multinuclear 3d–4f complexes from suitable building blocks is a promising strategy for the design of novel molecular magnetic architectures.

## ASSOCIATED CONTENT

### Supporting Information

Table of selected bond distances (Å) and angles (deg) and hydrogen bond parameters (Tables S1 and S2), and magnetic measurement (Figures S1–S7). This material is available free of charge via the Internet at <http://pubs.acs.org>.

## AUTHOR INFORMATION

### Corresponding Author

\*E-mail: tang@ciac.jl.cn.

### Notes

The authors declare no competing financial interest.

## ACKNOWLEDGMENTS

We thank the National Natural Science Foundation of China (Grants 91022009, 21241006, and 21221061) for financial support.

## REFERENCES

- (1) Christou, G.; Gatteschi, D.; Hendrickson, D. N.; Sessoli, R. *MRS Bull.* **2000**, 25, 66.
- (2) Ishikawa, N.; Sugita, M.; Ishikawa, T.; Koshihara, S.; Kaizu, Y. *J. Am. Chem. Soc.* **2003**, 125, 8694.
- (3) Osa, S.; Kido, T.; Matsumoto, N.; Re, N.; Pochaba, A.; Mrozinski, J. *J. Am. Chem. Soc.* **2004**, 126, 420.
- (4) Ako, A. M.; Hewitt, I. J.; Mereacre, V.; Clérac, R.; Wernsdorfer, W.; Anson, C. E.; Powell, A. K. *Angew. Chem., Int. Ed.* **2006**, 45, 5048.
- (5) Ako, A. M.; Mereacre, V.; Clerac, R.; Wernsdorfer, W.; Hewitt, I. J.; Anson, C. E.; Powell, A. K. *Chem. Commun.* **2009**, 544.
- (6) Zaleski, C. M.; Depperman, E. C.; Kampf, J. W.; Kirk, M. L.; Pecoraro, V. L. *Angew. Chem., Int. Ed.* **2004**, 43, 3912.
- (7) Karotsis, G.; Kennedy, S.; Teat, S. J.; Beavers, C. M.; Fowler, D. A.; Morales, J. J.; Evangelisti, M.; Dalgarno, S. J.; Brechin, E. K. *J. Am. Chem. Soc.* **2010**, 132, 12983.
- (8) Aronica, C.; Pilet, G.; Chastanet, G.; Wernsdorfer, W.; Jacquot, J.-F.; Luneau, D. *Angew. Chem., Int. Ed.* **2006**, 45, 4659.
- (9) Langley, S. K.; Ungur, L.; Chilton, N. F.; Moubaraki, B.; Chibotaru, L. F.; Murray, K. S. *Chem.—Eur. J.* **2011**, 17, 9209.
- (10) Ferbinteanu, M.; Kajiwar, T.; Choi, K.-Y.; Nojiri, H.; Nakamoto, A.; Kojima, N.; Cimpoesu, F.; Fujimura, Y.; Takaishi, S.; Yamashita, M. *J. Am. Chem. Soc.* **2006**, 128, 9008.
- (11) Xu, G.-F.; Gamez, P.; Tang, J.; Clérac, R.; Guo, Y.-N.; Guo, Y. *Inorg. Chem.* **2012**, 51, 5693.
- (12) Colacio, E.; Ruiz-Sanchez, J.; White, F. J.; Brechin, E. K. *Inorg. Chem.* **2011**, 50, 7268.
- (13) Ke, H.; Zhao, L.; Guo, Y.; Tang, J. *Inorg. Chem.* **2012**, 51, 2699.
- (14) Mondal, K. C.; Kostakis, G. E.; Lan, Y.; Wernsdorfer, W.; Anson, C. E.; Powell, A. K. *Inorg. Chem.* **2011**, 50, 11604.
- (15) Chandrasekhar, V.; Pandian, B. M.; Vittal, J. J.; Clérac, R. *Inorg. Chem.* **2009**, 48, 1148.
- (16) Mondal, K. C.; Sundt, A.; Lan, Y.; Kostakis, G. E.; Waldmann, O.; Ungur, L.; Chibotaru, L. F.; Anson, C. E.; Powell, A. K. *Angew. Chem., Int. Ed.* **2012**, 51, 7550.
- (17) Langley, S. K.; Chilton, N. F.; Ungur, L.; Moubaraki, B.; Chibotaru, L. F.; Murray, K. S. *Inorg. Chem.* **2012**, 51, 11873.
- (18) Bencini, A.; Benelli, C.; Caneschi, A.; Carlin, R. L.; Dei, A.; Gatteschi, D. *J. Am. Chem. Soc.* **1985**, 107, 8128.
- (19) Andruh, M.; Costes, J.-P.; Diaz, C.; Gao, S. *Inorg. Chem.* **2009**, 48, 3342.
- (20) Zheng, Y.-Z.; Evangelisti, M.; Winpenny, R. E. P. *Angew. Chem., Int. Ed.* **2011**, 50, 3692.
- (21) Peng, J.-B.; Zhang, Q.-C.; Kong, X.-J.; Ren, Y.-P.; Long, L.-S.; Huang, R.-B.; Zheng, L.-S.; Zheng, Z. *Angew. Chem., Int. Ed.* **2011**, 50, 10649.
- (22) Zheng, Y.-Z.; Evangelisti, M.; Tuna, F.; Winpenny, R. E. P. *J. Am. Chem. Soc.* **2011**, 134, 1057.
- (23) Peng, J.-B.; Zhang, Q.-C.; Kong, X.-J.; Zheng, Y.-Z.; Ren, Y.-P.; Long, L.-S.; Huang, R.-B.; Zheng, L.-S.; Zheng, Z. *J. Am. Chem. Soc.* **2012**, 134, 3314.
- (24) Dinca, A. S.; Ghirri, A.; Madalan, A. M.; Affronte, M.; Andruh, M. *Inorg. Chem.* **2012**, 51, 3935.
- (25) Dunbar, K. R. *Inorg. Chem.* **2012**, 51, 12055.
- (26) Ruiz, J.; Mota, A. J.; Rodriguez-Dieguez, A.; Titos, S.; Herrera, J. M.; Ruiz, E.; Cremades, E.; Costes, J. P.; Colacio, E. *Chem. Commun.* **2012**, 48, 7916.
- (27) Liu, C.-S.; Du, M.; Sanudo, E. C.; Echeverria, J.; Hu, M.; Zhang, Q.; Zhou, L.-M.; Fang, S.-M. *Dalton Trans.* **2011**, 40, 9366.
- (28) Bi, Y.; Wang, X.-T.; Liao, W.; Wang, X.; Deng, R.; Zhang, H.; Gao, S. *Inorg. Chem.* **2009**, 48, 11743.
- (29) Barron, L. D. *Nat. Mater.* **2008**, 7, 691.
- (30) Li, X.-L.; Chen, C.-L.; Gao, Y.-L.; Liu, C.-M.; Feng, X.-L.; Gui, Y.-H.; Fang, S.-M. *Chem.—Eur. J.* **2012**, 18, 14632.
- (31) Long, J.; Vallat, R.; Ferreira, R. A. S.; Carlos, L. D.; Almeida Paz, F. A.; Guari, Y.; Larionova, J. *Chem. Commun.* **2012**, 48, 9974.
- (32) Burrow, C. E.; Burchell, T. J.; Lin, P.-H.; Habib, F.; Wernsdorfer, W.; Clérac, R.; Murugesu, M. *Inorg. Chem.* **2009**, 48, 8051.
- (33) Novitchi, G.; Wernsdorfer, W.; Chibotaru, L. F.; Costes, J.-P.; Anson, C. E.; Powell, A. K. *Angew. Chem., Int. Ed.* **2009**, 48, 1614.
- (34) Wu, G.; Hewitt, I. J.; Mameri, S.; Lan, Y.; Clérac, R.; Anson, C. E.; Qiu, S.; Powell, A. K. *Inorg. Chem.* **2007**, 46, 7229.
- (35) Hosoi, A.; Yukawa, Y.; Igarashi, S.; Teat, S. J.; Roubeau, O.; Evangelisti, M.; Cremades, E.; Ruiz, E.; Barrios, L. A.; Aromí, G. *Chem.—Eur. J.* **2011**, 17, 8264.
- (36) Sessoli, R.; Powell, A. K. *Coord. Chem. Rev.* **2009**, 253, 2328.
- (37) Yang, X.; Chan, C.; Lam, D.; Schipper, D.; Stanley, J. M.; Chen, X.; Jones, R. A.; Holliday, B. J.; Wong, W.-K.; Chen, S.; Chen, Q. *Dalton Trans.* **2012**, 41, 11449.
- (38) Peng, J.-B.; Ren, Y.-P.; Kong, X.-J.; Long, L.-S.; Huang, R.-B.; Zheng, L.-S. *CrystEngComm* **2011**, 13, 2084.
- (39) Tanase, S.; Sottini, S.; Marvaud, V.; Groenen, E. J. J.; Chamoiseau, L.-M. *Eur. J. Inorg. Chem.* **2010**, 2010, 3478.
- (40) Yan, P.-F.; Lin, P.-H.; Habib, F.; Aharen, T.; Murugesu, M.; Deng, Z.-P.; Li, G.-M.; Sun, W.-B. *Inorg. Chem.* **2011**, 50, 7059.
- (41) Sheldrick, G. M. *Acta Crystallogr. Sect. A: Found. Crystallogr.* **2008**, 64, 112.
- (42) Boudreaux, E. A.; Mulay, L. N. *Theory and Applications of Molecular Paramagnetism*; John Wiley & Sons: New York, 1976.
- (43) Feng, W.; Zhang, Y.; Lu, X.; Hui, Y.; Shi, G.; Zou, D.; Song, J.; Fan, D.; Wong, W.-K.; Jones, R. A. *CrystEngComm* **2012**, 14, 3456.
- (44) Watanabe, A.; Yamashita, A.; Nakano, M.; Yamamura, T.; Kajiwar, T. *Chem.—Eur. J.* **2011**, 17, 7428.
- (45) Kajiwar, T.; Nakano, M.; Takahashi, K.; Takaishi, S.; Yamashita, M. *Chem.—Eur. J.* **2011**, 17, 196.
- (46) Gao, T.; Xu, L.-L.; Zhang, Q.; Li, G.-M.; Yan, P.-F. *Inorg. Chem. Commun.* **2012**, 26, 60.
- (47) Miyasaka, H.; Saitoh, A.; Abe, S. *Coord. Chem. Rev.* **2007**, 251, 2622.
- (48) Sakamoto, S.; Yamauchi, S.; Hagiwara, H.; Matsumoto, N.; Sunatsuki, Y.; Re, N. *Inorg. Chem. Commun.* **2012**, 26, 20.
- (49) Gao, Y. J.; Xu, G. F.; Zhao, L.; Tang, J.; Liu, Z. L. *Inorg. Chem.* **2009**, 48, 11495.
- (50) Xue, S.; Zhao, L.; Guo, Y.-N.; Chen, X.-H.; Tang, J. *Chem. Commun.* **2012**, 48, 7031.
- (51) Gass, I. A.; Moubaraki, B.; Langley, S. K.; Batten, S. R.; Murray, K. S. *Chem. Commun.* **2012**, 48, 2089.
- (52) Langley, S. K.; Moubaraki, B.; Murray, K. S. *Inorg. Chem.* **2012**, 51, 3947.
- (53) Vallejo, J.; Cano, J.; Castro, I.; Julve, M.; Lloret, F.; Fabelo, O.; Canadillas-Delgado, L.; Pardo, E. *Chem. Commun.* **2012**, 48, 7726.
- (54) Guo, Y.-N.; Chen, X.-H.; Xue, S.; Tang, J. *Inorg. Chem.* **2012**, 51, 4035.
- (55) Feltham, H. L. C.; Lan, Y.; Klöwer, F.; Ungur, L.; Chibotaru, L. F.; Powell, A. K.; Brooker, S. *Chem.—Eur. J.* **2011**, 17, 4362.
- (56) Costes, J.-P.; Dahan, F.; Dupuis, A.; Laurent, J.-P. *Chem.—Eur. J.* **1998**, 4, 1616.
- (57) Lin, P.-H.; Burchell, T. J.; Clérac, R.; Murugesu, M. *Angew. Chem., Int. Ed.* **2008**, 47, 8848.
- (58) Xue, S.; Zhao, L.; Guo, Y.-N.; Deng, R.; Guo, Y.; Tang, J. *Dalton Trans.* **2011**, 40, 8347.

- (59) Yamashita, A.; Watanabe, A.; Akine, S.; Nabeshima, T.; Nakano, M.; Yamamura, T.; Kajiware, T. *Angew. Chem., Int. Ed.* **2011**, *50*, 4016.
- (60) Maeda, M.; Hino, S.; Yamashita, K.; Kataoka, Y.; Nakano, M.; Yamamura, T.; Kajiware, T. *Dalton Trans.* **2012**, *41*, 13640.
- (61) Hino, S.; Maeda, M.; Yamashita, K.; Kataoka, Y.; Nakano, M.; Yamamura, T.; Nojiri, H.; Kofu, M.; Yamamuro, O.; Kajiware, T. *Dalton Trans.* **2013**, *42*, 2683.
- (62) Meng, Z.-S.; Guo, F.-S.; Liu, J.-L.; Leng, J.-D.; Tong, M.-L. *Dalton Trans.* **2012**, *41*, 2320.
- (63) Yu, W.-R.; Lee, G.-H.; Yang, E.-C. *Dalton Trans.* **2013**, *42*, 3941.